Inorg. Chem. **2007**, *46*, 10724–10735

Anion–π Interactions in Bisadenine Derivatives: A Combined Crystallographic and Theoretical Study

Angel Garcia-Raso,*,† Francisca M. Albertí,† Juan J. Fiol,† Andres Tasada,† Miquel Barceló-Oliver,† Elies Molins,‡ Daniel Escudero,† Antonio Frontera,*,† David Quiñonero,† and Pere M. Deyà*,†

Department of Chemistry, Universitat de les Illes Balears, Crta. de Valldemossa km 7.5, E-07122 Palma de Mallorca, Spain and Institut de Ciència de Materials de Barcelona (CSIC), Campus de la UAB, E-08193 Cerdanyola (Barcelona), Spain

Received August 3, 2007

In this manuscript we report a high-level ab initio study of anion–π interactions involving N^9-methyl-adenine, N^6-methyl-adenine, N^9-methyl-hypoxanthine, a dimer of N^9-methyl-adenine, and N^9,$N^{9'}$-trimethylene-bisadenine. DNA bases like adenine are electron-deficient arenes that are well suited for interacting favorably with anions. We demonstrate that these compounds are able to interact favorably with anions. N^9-Methyl-adenine, N^6-methyl-adenine, and the dimer of N^9-methyl-adenine interact with the anion via the six-membered ring more strongly than adenine due to cooperativity effects between the noncovalent π–π and anion–π interactions. This pattern, i.e., coexistence of π–π and anion–π bonding, is observed experimentally in the solid state. Finally, we report the solid-state characterization of two new compounds N^6,$N^{6'}$-dimethylene-bisadenine hydrochloride and an outer-sphere complex of protonated N^9,$N^{9'}$-trimethylene-bishypoxanthine with zinc tetrachloride anion, that exhibit interesting anion–π interactions. They are in strong agreement with high-level theoretical calculations.

1. Introduction

In modern chemistry, noncovalent interactions are decisive. This is especially true in the field of supramolecular chemistry and molecular recognition.[1] In particular, interactions involving aromatic rings[2] are key processes in both chemical and biological recognition since aromatic rings are omnipresent in biological systems. A classical example is the interaction of cations with aromatic systems, namely, cation$-\pi$ interactions,[3] which are supposed to be decisive in the ion selectivity of potassium channels.[4] Such interactions are also important for the binding of acetylcholine to the active site of the enzyme acetylcholine esterase.[5] Recently, the importance of cation$-\pi$ interactions in neurotransmitter receptors has been demonstrated,[6] and they play an important role in transport of nitrogen through the membrane by the ammonia transport protein.[7] Anion$-\pi$ interactions[8] are also important noncovalent forces that have attracted considerable attention in the last 4 years. They have been observed experimentally, supporting the theoretical predictions and promising proposal for use of anion receptors based on anion$-\pi$ interactions in molecular recognition.[9] Moreover, Berryman et al. reported structural criteria for the design of anion receptors based on the interaction of halides with electron-deficient arenes.[10] In addition, π-acidic oligonaphthalendiimide rods have been recently proposed as transmembrane anion$-\pi$ slides.[11] A recent review by P. Gamez et al. deals with anion-binding involving π-acidic

* To whom correspondence should be addressed. Fax: +34 971 173426. E-mail: toni.frontera@uib.es.
† Universitat de les Illes Balears.
‡ CSIC.

(1) Hunter, C. A.; Sanders, J. K. M. *J. Am. Chem. Soc.* **1990**, *112*, 5525.
(2) Meyer, E. A.; Castellano, R. K.; Diederich, F. *Angew. Chem., Int. Ed.* **2003**, *42*, 1210.
(3) (a) Ma, J. C.; Dougherty, D. A. *Chem. Rev.* **1997**, *97*, 1303. (b) Gallivan, J. P.; Dougherty, D. A. *Proc. Natl. Acad. Sci. U.S.A.* **1999**, *96*, 9459. (c) Gokel, G. W.; Wall, S. L. D.; Meadows, E. S. *Eur. J. Org. Chem.* **2000**, 2967. (d) Gokel, G. W.; Barbour, L. J.; Wall, S. L. D.; Meadows, E. S. *Coord. Chem. Rev.* **2001**, *222*, 127. (e) Gokel, G. W.; Barbour, L. J.; Ferdani, R.; Hu, J. *Acc. Chem. Res.* **2002**, *35*, 878. (f) Hunter, C. A.; Singh, J.; Thorton, J. M. *J. Mol. Biol.* **1991**, *218*, 837.
(4) (a) Kumpf, R. A.; Dougherty, D. A. *Science* **1993**, *261*, 1708. (b) Heginbotham, L.; Lu, Z.; Abramson, T.; Mackinnon, R. *Biophys. J.* **1994**, *66*, 1061.
(5) Dougherty, D. A. *Science* **1996**, *271*, 163.
(6) Lummis, S. C. R.; Beene, D. L.; Harrison, N. J.; Lester, H. A.; Dougherty, D. A. *Chem. Biol.* **2005**, *12*, 993.
(7) Ishikita, H.; Knapp, E.-W. *J. Am. Chem. Soc.* **2007**, *129*, 1210.
(8) (a) Quiñonero, D.; Garau, C.; Rotger, C.; Frontera, A.; Ballester, P.; Costa, A.; Deyà, P. M. *Angew. Chem., Int. Ed.* **2002**, *41*, 3389. (b) Alkorta, I.; Rozas, I.; Elguero, J. *J. Am. Chem. Soc.* **2002**, *124*, 8593. (c) Mascal, M.; Armstrong, A.; Bartberger, M. *J. Am. Chem. Soc.* **2002**, *124*, 6274.

10.1021/ic701555n CCC: $37.00
Published on Web 11/14/2007

Chart 1. Structure and IUPAC Atom Numbering of the 9H-Adenine Tautomer

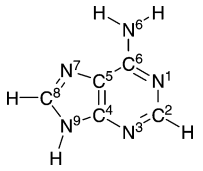

heteroaromatic rings.[12] Last, $\pi-\pi$ interactions[13] are weak noncovalent forces that play an essential role in the folding of proteins,[14] in the structure of DNA, as well as in its interactions with small molecules.[15] They are widely used in supramolecular chemistry and very important binding forces that determine the packing of organic molecules in crystals. They are also used in crystal engineering for the design of functional materials.[16]

Many π-acidic aromatic rings can be found in biomolecules, among them the DNA bases are representative. It is well known that the $\pi-\pi$ stacking interactions between the bases stabilize the DNA double helix. In addition, there is experimental evidence of attractive anion−base interactions, including the six-membered rings of adenine (Chart 1), guanine, and thymine.[12,17] Therefore, it is feasible that both interactions coexist in a given biological system. Some of us have recently published that cooperativity effects exist between $\pi-\pi$ and anion$-\pi$ interactions.[18] Actually, we demonstrated that when either an anion or a cation interacts with an aromatic ring establishing a cation/anion$-\pi$ interaction, the strength of the interaction is stronger if the aromatic ring is involved in a $\pi-\pi$ stacking interaction. In addition some of us have communicated the synthesis and X-ray characterization of N^9,$N^{9'}$-trimethylene-bisadenine complexes with tetrachlorometalates ($ZnCl_4^{2-}$, $HgCl_4^{2-}$) and an inner-sphere complex of N^6,$N^{6'}$-trimethylene-bisadenine with trichlorozincate anion.[19] In this manuscript, we study and compare, using theoretical methods, the capability of N^9-methyl-adenine, **1**, N^6-methyl adenine, **2**, N^9-methyl-hypoxanthine, **3**, a dimer of N^9-methyl-adenine, **4**, and N^9,$N^{9'}$-trimethylene-bisadenine, **5**, to interact with chloride anion. We also explore the existence of synergistic effects between anion$-\pi$ and $\pi-\pi$ interactions in these systems (see Figure 1, top). Moreover, we analyze the solid-state structures of one inner-sphere complex of N^6,$N^{6'}$-trimethylene-bisadenine with $ZnCl_3^-$, **6**, and the outer-sphere complexes of N^9,$N^{9'}$-trimethylene-bisadenine with $ZnCl_4^{2-}$, **7**, and $HgCl_4^{2-}$, **8**. In the latter complexes the coexistence of both $\pi-\pi$ and anion$-\pi$ interactions is evident and an important factor in determining the crystal packing. An anion$-\pi$ interaction is also found in the crystal structure of the inner-sphere complex of N^6,$N^{6'}$-trimethylene-bisadenine, **6**. We also report the synthesis and X-ray characterization of N^6,$N^{6'}$-dimethylene-bisadenine dihydrochloride, **9**, and an outer-sphere complex of N^9,$N^{9'}$-trimethylene-bishypoxanthine with $ZnCl_4^{2-}$, **10**, that also exhibit illustrative anion$-\pi$ interactions.

Study of the binding ability of N^9-methyl-adenine, **1**, N^6-methyl-adenine, **2**, the dimer of N^9-methyl-adenine, **4**, N^9,$N^{9'}$-trimethylene-bisadenine, **5**, and N^9-methyl-hypoxanthine, **3**, toward Cl^- anion has been performed using high-level ab initio calculations, including utilization of the molecular interaction potential with polarization (MIPp)[20] calculation of compounds **1**−**5**. The MIPp is a convenient tool for predicting binding properties. It has been successfully used for rationalizing molecular interactions such us hydrogen bonding and ion$-\pi$ interactions and predicting molecular reactivity.[21] The MIPp partition scheme is an improved generalization of the MEP where three terms contribute to the interaction energy: (i) an electrostatic term identical to the MEP,[22] (ii) a classical dispersion-repulsion term,[23] and (iii) a polarization term derived from perturbational theory.[24]

2. Theoretical Methods

The geometries of all compounds studied in this work were fully optimized using the RI-MP2/6-31++G** level of theory within the program TURBOMOLE version 5.7.[25] The RI-MP2 method[26] applied to the study of cation$-\pi$ and anion$-\pi$ interactions is

(9) (a) Demeshko, S.; Dechert, S.; Meyer, F. *J. Am. Chem. Soc*. **2004**, *126*, 4508. (b) Schottel, B. L.; Bacsa, J.; Dunbar, K. R. *Chem. Commun*. **2005**, 46. (c) Rosokha, Y. S.; Lindeman, S. V.; Rosokha, S. V.; Kochi, J. K. *Angew. Chem., Int. Ed*. **2004**, *43*, 4650. (d) de Hoog, P.; Gamez, P.; Mutikainen, I.; Turpeinen, U.; Reedijk, J. *Angew. Chem., Int. Ed*. **2004**, *43*, 5815. (e) Frontera, A.; Saczewski, F.; Gdaniec, M.; Dziemidowicz-Borys, E.; Kurland, A.; Deyà, P. M.; Quiñonero, D.; Garau, C. *Chem. Eur. J*. **2005**, *11*, 6560. (f) Gil-Ramirez, G.; Benet-Buchholz, J.; Escudero-Adan, E. C.: Ballester, P. *J. Am. Chem. Soc*. **2007**, *129*, 3820.

(10) Berryman, O. B.; Bryantsev, V. S.; Stay, D. P.; Johnson, D. W.; Hay, B. P. *J. Am. Chem. Soc*. **2007**, *129*, 48.

(11) (a) Gorteau, V.; Bollot, G.; Mareda, J.; Perez-Velasco, A.; Matile, S. *J. Am. Chem. Soc*. **2006**, *128*, 14788. (b) Gorteau, V.; Bollot, G.; Mareda, J.; Matile, S. *Org. Biomol. Chem*. **2007**, *5*, 3000.

(12) Gamez, P.; Mooibroek, T. J.; Teat, S. J.; Reedijk, J. *Acc. Chem. Res*. **2007**, *40*, 435.

(13) Hunter, C. A. *Chem. Soc. Rev*. **1994**, *23*, 101.

(14) Bhattacharyya, R.; Samanta, U.; Chakrabarti, P. *Protein Eng*. **2002**, *15*, 91 and references therein.

(15) (a) Gurrath, M.; Müller, G.; Höltje, H.-D. *Perspect. Drug Discovery Des*. **1998**, *12*, 135. (b) Vedani, A.; Zbinden, P.; Snyder, J. P.; Greenidge, P. A. *J. Am. Chem. Soc*. **1995**, *117*, 4987.

(16) Desiraju, G. R. *Angew. Chem., Int. Ed. Engl*. **1995**, *34*, 2311.

(17) (a) Suzuki, T.; Hirai, Y.; Monjushiro, H.; Kaizaki, S. *Inorg. Chem*. **2004**, *43*, 6435. (b) Price, C.; Shipman, M. A.; Rees, N. H.; Eisegood, M. R. J.; Edwards, A. J.; Clegg, W.; Houlton, A. *Chem. Eur. J*. **2001**, *7*, 1194. (c) Suksangpanya, U.; Blake, A. J.; Hubberstey, P.; Wilson, C. *Cyst. Eng. Commun*. **2004**, *8*, 70.

(18) (a) Frontera, A.; Quiñonero, D.; Costa, A.; Ballester, P.; Deyà, P. M. *New J. Chem*. **2007**, *31*, 556. (b) Quiñonero, D.; Frontera, A.; Garau, C.; Costa, A.; Ballester, P.; Deyà, P. M. *ChemPhysChem* **2006**, *7*, 2487.

(19) (a) García-Raso, A.; Fiol, J. J.; Bádenas, F.; Solans, X.; Font-Bardia, M. *Polyhedron* **1999**, *18*, 765. (b) García-Raso, A.; Fiol, J. J.; Bádenas, F.; Solans, X.; Font-Bardia, M. *Polyhedron* **1999**, *18*, 3077. (c) García-Raso, A.; Fiol, J. J.; Bádenas, F.; Tasada, A.; Solans, X.; Font-Bardia, M.; Basallote, M.; Fernández-Trujillo, M. J.; Sánchez, D. *J. Inorg. Biochem*. **2003**, *93*, 141. (d) García-Raso, A.; Fiol, J. J.; Tasada, A.; Albertí, F. M.; Bádenas, F.; Solans, X.; Font-Bardia, M. *Polyhedron* **2007**, *26*, 949.

(20) Luque, F. J.; Orozco, M. *J. Comput. Chem*. **1998**, *19*, 866.

(21) (a) Hernández, B.; Orozco, M.; Luque, F. J. *J. Comput.-Aided Mol. Des*. **1997**, *11*, 153. (b) Luque, F. J.; Orozco, M. *J. Chem. Soc., Perkin Trans 2* **1993**, 683. (c) Quiñonero, D.; Frontera, A.; Suñer, G. A.; Morey, J.; Costa, A.; Ballester, P.; Deyà, P. M. *Chem. Phys. Lett*. **2000**, *326*, 247. (d) Quiñonero, D.; Frontera, A.; Garau, C.; Ballester, P.; Costa, A.; Deyà, P. M. *Chem. Phys. Chem*. **2006**, *7*, 2487.

(22) Scrocco, E.; Tomasi, J. *Top. Curr. Chem*. **1973**, *42*, 95.

(23) Orozco, M.; Luque, F. J. *J. Comput. Chem*. **1993**, *14*, 587.

(24) Francl, M. M. *J. Phys. Chem*. **1985**, *89*, 428.

(25) Ahlrichs, R.; Bär, M.; Hacer, M.; Horn, H.; Kömel, C. *Chem. Phys. Lett*. **1989**, *162*, 165.

(26) (a) Feyereisen, M. W.; Fitzgerald, G.; Komornicki, A. *Chem. Phys. Lett*. **1993**, *208*, 359. (b) Vahtras, O.; Almlof, J.; Feyereisen, M. W. *Chem. Phys. Lett*. **1993**, *213*, 514.

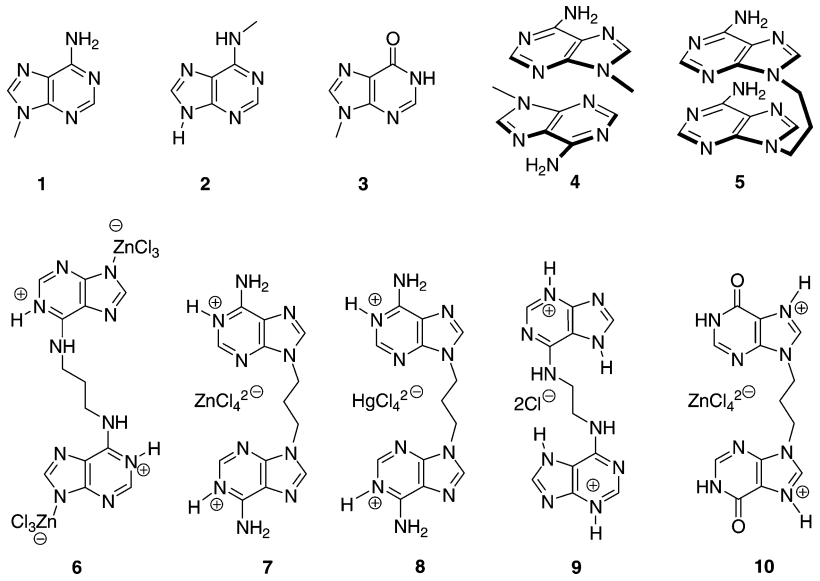

Figure 1. N^9-methyl-adenine ($AdeCH_3$), **1**, N^6-methyl-adenine ($AdeNHCH_3$), **2**, N^9-methyl-hypoxanthine ($HypCH_3$), **3**, dimer of N^9-methyl-adenine, **4**, N^9,$N^{9'}$-trimethylene-bisadenine $[(Ade)_2(CH_2)_3]$, **5**, $[(H\text{-}AdeNH)_2(CH_2)_3(ZnCl_3)_2]$, **6**, $[(H\text{-}Ade)_2(CH_2)_3][ZnCl_4]$, **7**, $[(H\text{-}Ade)_2(CH_2)_3][HgCl_4]$, **8**, $[(H\text{-}AdeNH)_2(CH_2)_2][2Cl]$, **9**, and $[(H\text{-}Hyp)_2(CH_2)_3][ZnCl_4]$, **10**.

considerably faster than the MP2, and the interaction energies and equilibrium distances are almost identical for both methods.[27] The binding energies were calculated with correction for the basis set superposition error (BSSE) using the Boys−Bernardi counterpoise technique.[28] This methodology (RI-MP2) has been successfully used for computation of stacking energies of DNA bases[29] and study of a variety of intermolecular interactions, such as N−H···π interactions[30] and dihydrogen with aromatic systems.[31] Moreover, there are several works that have successfully used RI-MP2 calculations to study several issues regarding nucleic acid bases, i.e., stacking,[29,32] hydrogen bonding,[33] tautomers,[34] and complexation with metal ions.[35] Optimization of the complexes has been performed without imposing symmetry constrains unless otherwise noted. In Table 1 we summarize and compare the interaction energies and equilibrium distances of anion−π complexes of chloride with several π-acidic rings computed at the MP2/6-31++G** and RI-MP2/6-31++G** levels of theory. The results indicate that that the interaction energies and equilibrium distances obtained at both levels of theory are in excellent agreement, giving reliability to the RI approximation. Calculation of the MIPp maps of **1**−**5** interacting with Cl^- was performed using the HF wavefunction and the RI-MP2/6-31++G** geometries computed from Gaussian 03 package[36] by means of the MOPETE-98 program.[37] The ionic van der Waals parameters for Cl^- were taken from the literature.[38] Some basic concepts of MIPp follow (see refs 20 and 23 for a more comprehensive treatment). The MEP can be understood as the interaction energy between the molecular charge distribution and a classical point charge. The formalism used to derive MEP remains valid for any classical charge; therefore, it can be generalized using eq 1

$$\mathrm{MEP} = \sum_A \frac{Z_A Q_B}{|R_B - R_A|} - \sum_i^{occ} \sum_\mu \sum_\nu c_{\mu i} c_{\nu i} < \phi_\mu | \frac{Q_B}{|R_B - r|} | \phi_\nu > \quad (1)$$

where Q_B is the classical point charge at R_B. Q_B can adopt any value, but it has a chemical meaning only when $Q_B = 1$ (proton); ϕ is set of basis functions used for the quantum mechanical molecule A, $c_{\mu i}$ is the coefficient of atomic orbital μ in the molecular orbital i

The MEP formalism permits the rigorous computation of the electrostatic interaction between any classical particle and the molecule. Nevertheless, nuclear repulsion and dispersion effects are omitted. This can be resolved by addition of a classical dispersion−repulsion term, which leads to the definition of MIP[23] (eq 2)

$$\mathrm{MIP} = \mathrm{MEP} + \sum_{A'B'} \left(\frac{C_{A'B'}}{|R_{B'} - R_{A'}|^{12}} - \frac{D_{A'B'}}{|R_{B'} - R_{A'}|^{6}} \right) \quad (2)$$

where C and D are empirical van der Waals parameters.

Table 1. Interaction Energies (kJ/mol) at the MP2(fu)/6-31++G** and RI-MP2(fu)/6-31++G** Levels of Theory with (E_{CP}, kJ/mol) and without (E, kJ/mol) the BSSE Correction and Equilibrium Distances (R_e, Å) for Several Complexes; MIP_P Energetic Values (kJ/mol) Obtained for the Different Arenes Interacting with Cl^- Are Also Included

	E		E_{CP}		R_e		
complex	MP2	RI-MP2	MP2	RI-MP2	MP2	RI-MP2	MIPp
$C_6F_6\cdots Cl^-$	−76.5	−76.9	−55.2	−54.8	3.155	3.154	−66.0
$C_6H_3F_3\cdots Cl^-$	−37.6	−37.6	−20.1	−20.1	3.332	3.336	−31.4
s-triazine$\cdots Cl^-$	−37.6	−37.6	−21.7	−22.2	3.223	3.220	−32.2
s-tetrazine$\cdots Cl^-$	−66.9	−66.9	−44.7	−44.7	2.890	2.890	−69.0
isocyanuric$\cdots Cl^-$	−95.3	−95.7	−70.2	−69.0	2.877	2.878	−96.6
$C_6H_6\cdots C_6H_6$	−20.9	−20.9	−5.4	−5.4	3.800	3.800	

(27) (a) Frontera, A.; Quiñonero, D.; Garau, C.; Ballester, P.; Costa, A.; Deyà, P. M. *J. Phys. Chem. A* **2005**, *109*, 4632. (b) Quiñonero, D.; Garau, C.; Frontera, A.; Ballester, P.; Costa, A.; Deyà, P. M. *J. Phys. Chem. A* **2006**, *110*, 5144.

(28) Boys, S. B.; Bernardi, F. *Mol. Phys*. **1970**, *19*, 553.

(29) Jurecka, P.; Hobza, P. *J. Am. Chem. Soc.* **2003**, *125*, 15608.

(30) Braun, J.; Neusser, H. J.; Hobza, P. *J. Chem. Phys. A* **2003**, *107*, 3918.

(31) Hübner, O.; Glöss, A.; Fichtner, M.; Klopper, W. *J. Chem. Phys. A* **2004**, *107*, 3019.

(32) Hobza, P.; Sponer, J. *J. Am. Chem. Soc*. **2002**, *124*, 11802.

(33) Sponer, J.; Jurecka, P.; Hobza, P. *J. Am. Chem. Soc*. **2003**, *126*, 10142.

(34) Trygubenko, S. A.; Bogdan, T. V.; Rueda, M.; Orozco, M.; Luque, F. J.; Sponer, J.; Slavicek, P.; Hobza, P. *Phys. Chem. Chem. Phys*. **2002**, *4*, 4192.

(35) Rusilek, L.; Sponer, J. *J. Phys. Chem. B* **2003**, *107*, 1913.

(36) Frisch, M. J.; et al. *Gaussian 03*; Gaussian, Inc.: Pittsburgh, PA, 2003.

(37) Luque, F. J.; Orozco, M. *MOPETE-98 computer program*; Universitat de Barcelona: Barcelona, 1998.

(38) Clark, M.; Cramer, R. D., III; Opdenbosch, N. *J. Comput. Chem*. **1989**, *10*, 982.

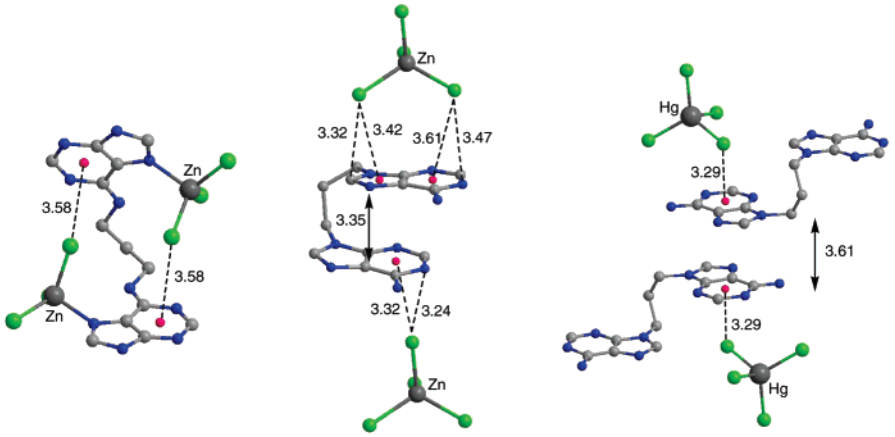

6 **7** **8**

Figure 2. Partial view of the X-ray structures of compounds **6**−**8**. The hydrogen atoms and water molecules are omitted for clarity. Distances in Ångstroms.

The definition of MIPp is given by eq 3

$$\mathrm{MIP_p} = MIP + \sum_{j}^{vir}\sum_{i}^{occ}\frac{1}{\epsilon_i - \epsilon_j}\left\{\sum_{\mu}\sum_{\nu} c_{\mu i}c_{\nu i} < \phi_\mu \left|\frac{Q_B}{|R_B - r|}\right| \phi_\nu > \right\}^2 \quad (3)$$

where polarization effects are included at the second-order perturbation level;[24] ϵ is the energy of virtual (j) and occupied (i) molecular orbitals. It is worth noting that eq 3 includes three important contributions: first, the rigorous calculation of electrostatic interactions between quantum mechanical and classical particles, second, introduction of an empirical dispersion−repulsion term, and third, the perturbative treatment of the polarization term.

In Table 1, we also included the interaction energies of π-acidic rings with Cl^- computed using the MIPp partition scheme. The agreement between the MP2 (without BSSE correction) and MIPp energies is good, taking into account that MIPp energies are obtained using the HF wavefunction of the isolated aromatic compound and Cl^- is treated as a classical particle.

3. Results and Discussion

3.1. X-ray Structures. As stated in the Introduction, some of us have previously communicated the synthesis and X-ray characterization of several inner- and outer-sphere complexes of $N^6,N^{6'}$- and $N^9,N^{9'}$-trimethylene-bisadenine with MCl_2 [M = Zn(II) and Hg(II)]; some of them are highlighted in Figure 2 (**6**−**8**). It is worth mentioning that in the solid state they exhibit interesting and relevant anion−π interactions, which were originally unnoticed.[19] In all cases, anion−π interactions, among others, determine the geometric features of the compounds in the solid state. In the inner-sphere complex **6** two intramolecular anion−π interactions stabilize the conformation of the bis-adenine in the solid state (see Figure 2). More interestingly, the X-ray structures of compounds **7** and **8** reveal a coexistence of two noncovalent interactions. In both outer-sphere complexes, the adenine participates in an anion−π interaction with the MCl_4^{2-} (M = Zn, Hg) anion and simultaneously is establishing a $\pi-\pi$ stacking interaction with another adenine. In compound **7** the $\pi-\pi$ stacking interaction is intramolecular and there are two nonequivalent $ZnCl_4^{2-}$ anions in the solid state that participate in anion−π interactions. One interaction involves two chlorine atoms of the anion: one interacting with the five-membered ring and the other interacting with the six-membered ring of the adenine. The other $ZnCl_4^{2-}$anion establishes the anion−π interaction using only one chlorine atom, which interacts with the six-membered ring of the second adenine. In contrast to compound **7**, the stacking interaction in compound **8** is intermolecular and the anion−π interaction only involves the six-membered ring (see Figure 2). It is worth mentioning that the pattern of the $\pi-\pi$ stacking interaction is different for compounds **7** and **8**. The former has a parallel displaced stacking where the six-membered ring of one adenine is over the six-membered ring of the other adenine. The latter has a parallel displaced stacking where the six-membered ring of one adenine is over the five-membered ring of the other adenine. Later on we demonstrate that both stacking modes have an active influence upon the anion−π interaction, which strengthens as a consequence of the $\pi-\pi$ stacking.

Scheme 1. Synthetic Procedure of Compounds **9** and **10**

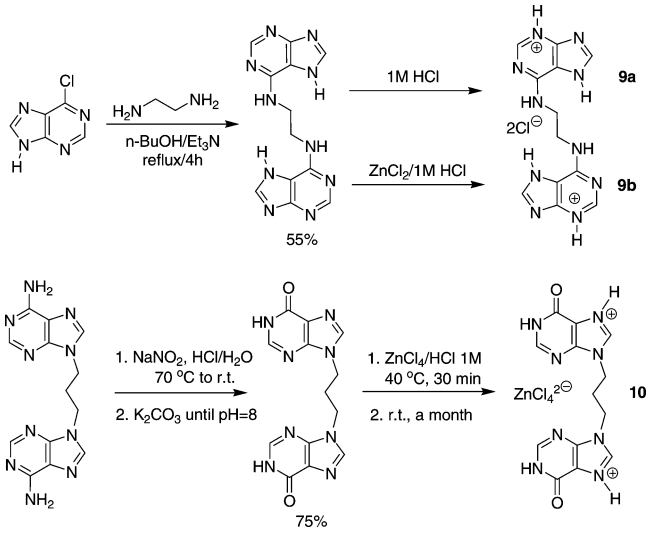

We synthesized two new compounds, **9** and **10**, using the following procedures as shown in Scheme 1. The precursor of **9**, $N^6,N^{6'}$-dimethylene-bisadenine, is easily prepared, in good yield (55%), from 6-chloropurine and 1,2-ethylenediamine under refluxing conditions in *n*-BuOH/Et_3N. Dissolution of this compound in 1 M HCl yields the corresponding

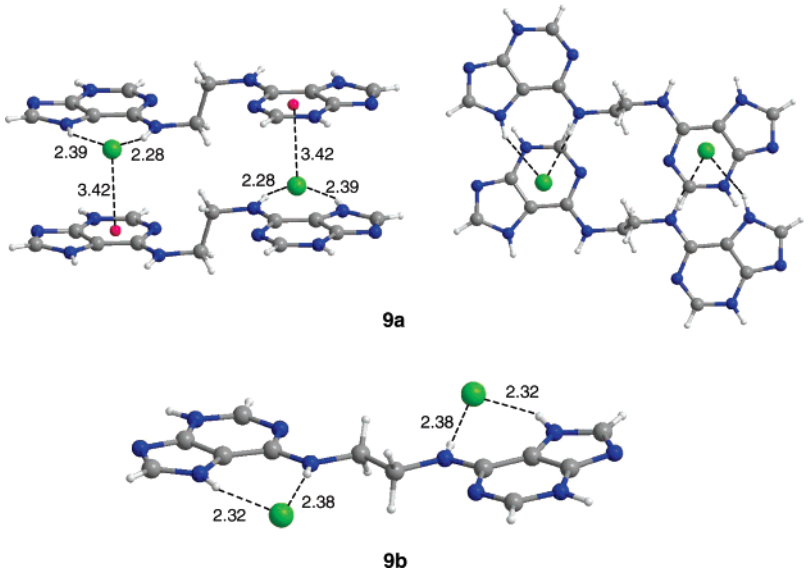

Figure 3. (Top) On-top (left) and perspective (right) views of the X-ray structure of the isomorphic form **9a**. (Bottom) Perspective view of the isomorphic form of **9b**, where anion$-\pi$ interactions are absent. Distances in Ångstroms.

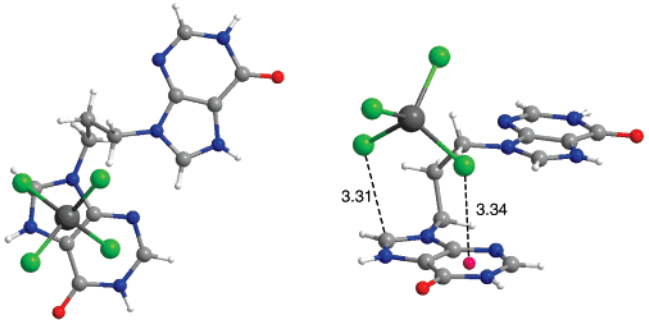

Figure 4. On-top and perspective views of the X-ray structure of compound **10**. The water molecules are omitted for clarity. Distances in Ångstroms.

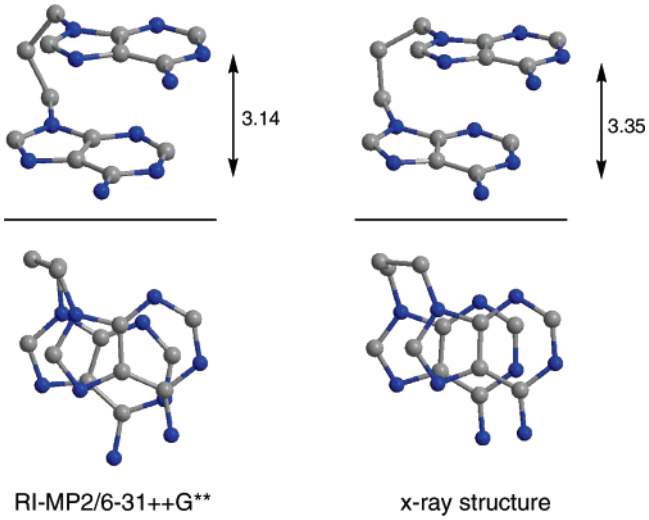

Figure 5. (Left) RI-MP2/6-31++G**-optimized structure of **5**. (Right) Partial view of the X-ray structure of compound **7**. The zenithal views of both structures are shown in the bottom. Distances in Ångstroms. The hydrogen atoms have been omitted for clarity.

hydrochloride **9a**.[19c] On the other hand, N^9,N^9-trimethylene-bishypoxanthine, precursor of **10**, is obtained in good yield (80%) by means oxidation of N^9,$N^{9'}$-trimethylene-bisadenine **5**, dissolved in acidic medium, using $NaNO_2$ as oxidizing

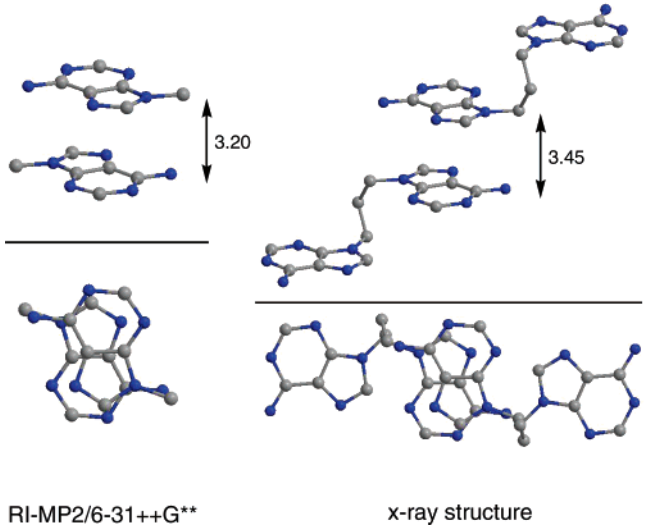

Figure 6. (Left) RI-MP2/6-31++G**-optimized structure of **4**. (Right) Partial view of the X-ray structure of compound **8**. The zenithal views of both structures are shown in the bottom. Distances in Ångstroms. The hydrogen atoms have been omitted for clarity.

agent. Compound **10** is obtained after treatment of N^9,N^9-trimethylene-bishypoxanthine with $ZnCl_2$ in HCl (1 M) at 40 °C. Crystals suitable for X-ray crystallography were obtained after 1 month.

The solid-state structure of complex **9** is shown in Figure 3. We obtained two isomorphic X-ray structures. One of them (**9a**) is obtained following the aforementioned synthetic procedure, and its solid-state structure is depicted in the top part of Figure 3. The chloride anion interacts via hydrogen bonding with two NH groups of the adenine moiety, corresponding to N^6 and N^7. Moreover, the anion is also involved in an anion$-\pi$ interaction, which is an important binding motif in the crystal since it holds together two bisadenine molecules. The second isomorphic structure (**9b**) is obtained when the N^6,$N^{6'}$-dimethylene-bisadenine is dissolved in HCl (1 M), mixed with $ZnCl_2$ at 40 °C for 30 min, and then allowed to stay at room temperature in an attempt

Scheme 2. Interaction Energies (kJ/mol) of Two Dimers of **1**, Bisadenine and Bishypoxanthine[a]

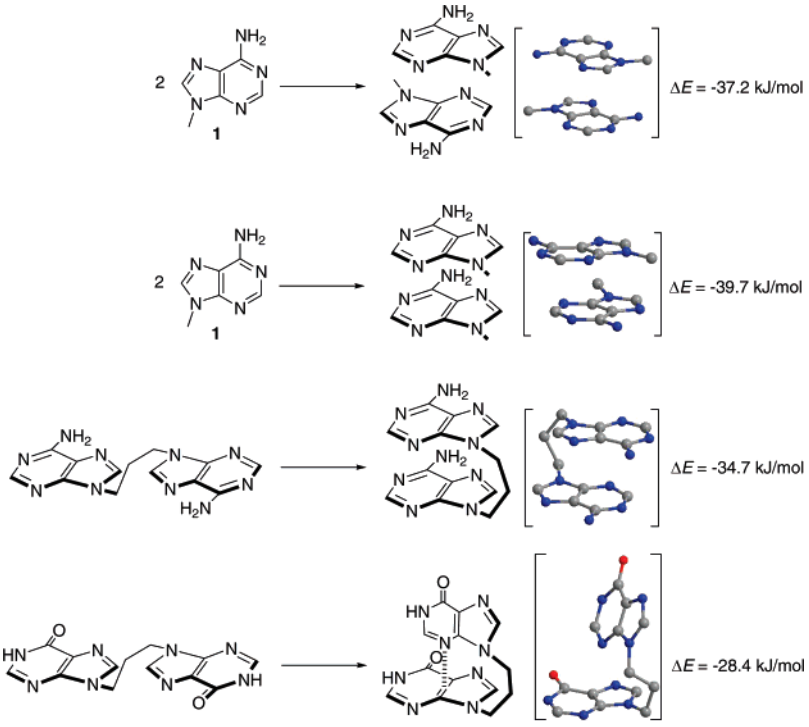

[a] In square brackets we represent the RI-MP2/6-31++G**-optimized structures.

to obtain a similar complex to **6** but with the corresponding dimethylene-bisadenine. In these conditions, crystals of **9b** grow with the geometry present in the bottom part of Figure 3. In this structure, anion−π interactions are not present and the Cl^- interacts with the adenine only through formation of hydrogen bonds with two NH groups. In contrast to the other isomorphic structure (**9a**), the adenine rings and both carbon atoms of the dimethylene bridge are almost coplanar. In both isomorphic structures the adenine moiety does not participate in π−π stacking interactions.

The solid-state structure of bishypoxanthine **10** is represented in Figure 4. One chlorine atom of the anion is forming an anion−π interaction with the six-membered ring of one hypoxanthine and another chlorine atom π-interacts mainly with one carbon atom of the five-membered ring. This binding mode is similar to the one described in complex **7**. In this structure, π−π stacking interactions between the hypoxanthine rings are not observed.

3.2. Energetic Analysis. We fully optimized compounds **1**−**5** at the RI-MP2/6-31++G** level in order to study their energetic affinity toward chlorine. In addition, compounds **4** and **5** are useful to analyze the stacking interaction modes observed in the X-ray structures of compounds **7** and **8**. We used the dimer of adenine **4** as a model of the intermolecular π−π stacking interaction present in the X-ray structure of **8** in order to keep the calculation affordable. We compared the geometric features of **4** and **5** to the X-ray structures, as shown in Figures 5 and 6. The agreement between the optimized and experimental structures regarding the relative disposition of the molecules in the stacking interaction is remarkable, especially in **4**, giving reliability to the theoretical level and model. We also computed compound **5** in a conformation where the arenes are not stacked in order to compare their relative stability and importance of the stacking interaction. The difference in energy between both conformers is 34.7 kJ/mol (see Scheme 2), indicating that the π−π stacking interaction is important. A parallel finding is obtained for **4**; the formation energy of the dimer is −37.2 kJ/mol, considerably more stable than that computed for the benzene dimer at the same level (−5.4 kJ/mol),[18a] indicating that the stacking interaction in **4** is very favored. For comparison purposes, we also computed the formation energy of the dimer of **1** in another orientation, where the six-membered ring of one adenine is located over the six-membered ring of the other adenine. Both dimers have very similar formation energies and equilibrium distances. Consequently, the stacking mode observed in **8**, where the five-membered ring of one adenine is over the six-membered ring of the other and vice versa, can be considered as a strong binding motif of the crystal structure. In addition, we studied the π−π stacking behavior of bishypoxhantine (bottom part of Scheme 2). In this case the π−π parallel stacking is probably not favored since we did not find a minimum on the potential-energy surface. Instead, we found a minimum energy structure that corresponds to a T-shaped stacking mode that is 28.4 kJ/mol lower in energy than the open conformer. It is worth noting that the parallel π−π stacking motif is not found in the crystal structure of bishypoxanthine **10**, in agreement with the theoretical results. Furthermore, the T-shaped stacking geometry implies a lone pair−π interaction between one nitrogen atom of the six-membered ring of one hypoxanthine moiety and the π system of the other. A likely explanation is that the π acidity of hypoxanthine is higher than adenine as a consequence of the carbonyl group that favors the interaction with the lone pair of the nitrogen atom.

Table 2. Contributions to the Total Interaction Energy (kJ/mol) Calculated with MIPp for **1**−**5** Interacting with Cl^- at Several Distances (Å) from the Center of the Rings

	E_e		E_p		E_{vw}		E_t	
distance	6R	5R	6R	5R	6R	5R	6R	5R
				1				
2.5	21.82	*8.32*	−59.57	*−61.91*	49.74	*62.32*	12.04	*8.78*
3.0	19.56	*6.77*	−35.45	*−36.28*	−4.06	*−3.26*	−19.94	*−32.77*
3.2	18.27	*6.02*	−29.18	*−29.76*	−6.90	*−6.73*	−17.81	*−30.51*
3.5	15.51	*4.56*	−20.23	*−20.57*	−6.65	*−6.77*	−11.33	*−22.74*
4.0	12.37	*3.09*	−13.25	*−13.46*	−4.43	*−4.51*	−5.31	*−14.88*
				2				
2.5	22.57	*10.99*	−65.25	*−67.13*	77.54	*114.91*	35.11	*58.77*
3.0	21.53	*10.24*	−38.75	*−38.62*	−1.17	*2.88*	−18.39	*−25.50*
3.2	20.36	*9.74*	−31.85	*−31.48*	−5.98	*−3.97*	−17.43	*−25.75*
3.5	18.48	*8.78*	−24.08	*−23.58*	−7.06	*−6.23*	−12.67	*−20.98*
4.0	15.34	*7.11*	−15.59	*−15.09*	−5.14	*−4.72*	−5.39	*−12.71*
				3				
2.5	−12.37	*13.08*	−65.29	*−67.97*	79.09	*109.01*	1.38	*54.13*
3.0	−5.06	*11.62*	−38.29	*−39.25*	−1.05	*1.34*	−44.39	*−26.29*
3.2	−3.39	*10.78*	−31.31	*−32.02*	−5.94	*−5.14*	−40.63	*−26.33*
3.5	−1.59	*9.57*	−23.49	*−23.95*	−7.11	*−7.02*	−32.19	*−21.40*
4.0	0.08	*7.77*	−15.09	*−15.34*	−5.14	*−5.23*	−20.15	*−12.79*
				4				
2.5	28.01	*18.10*	−68.34	*−68.93*	50.33	*57.93*	9.95	*7.11*
3.0	23.83	*15.68*	−41.05	*−41.26*	−4.97	*−4.51*	−22.20	*−30.10*
3.2	22.03	*14.55*	−33.86	*−34.15*	−7.82	*−7.69*	−19.65	*−27.30*
3.5	19.48	*14.55*	−25.96	*−34.15*	−7.77	*−7.69*	−14.25	*−27.30*
4.0	17.14	*11.50*	−20.19	*−20.31*	−6.40	*−6.48*	−9.45	*−15.30*
				5				
2.5	27.17	*13.54*	−76.54	*−85.73*	85.86	*157.04*	36.53	*84.85*
3.0	24.16	*11.62*	−45.73	*−50.08*	−1.17	*5.06*	−22.70	*−32.98*
3.2	22.49	*10.87*	−37.70	*−41.05*	−6.48	*−4.43*	−21.69	*−34.61*
3.5	19.90	*9.15*	−28.67	*−30.97*	−7.73	*−7.73*	−16.51	*−29.55*
4.0	15.84	*6.56*	−18.81	*−20.19*	−5.64	*−6.06*	−8.61	*−19.69*

Once it was demonstrated that the $\pi-\pi$ stacking interactions observed in the crystal are important and that the theoretical level is adequate to describe them, we computed the interaction of chloride with compounds **1**−**5** using the MIPp methodology. We obtained the MIPp interaction energies when a chloride anion approaches an adenine (or hypoxanthine) molecule perpendicular to the center of the six- and five-membered rings for compounds **1**−**5**, which are summarized in Table 2. The present and previous studies[8a,9e,39] demonstrate that the MIPp energies are in good agreement with the interaction energies calculated optimizing the complexes at the MP2 level of theory, which give reliability to the MIPp partition scheme. These calculations allow us to compare the $Cl^-\cdots\pi$ interactions of compounds **1**−**5** and learn if the ability of adenine for interacting with anions is improved when it is forming a stacking interaction with other adenine in any of the two stacking modes observed in the crystals of compounds **7** and **8**. The values in italics shown in Table 2 correspond to the interaction with the five-membered ring (5R). From inspection of the results, several

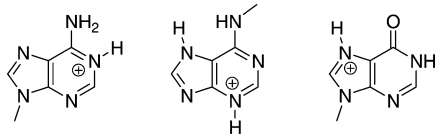

H-1 **H-2** **H-3**

Figure 7. Protonated forms of compounds **1**−**3** in positions N^1 (**H-1**), N^3 (**H-2**), and N^7 (**H-3**).

Table 3. Contributions to the Total Interaction Energy (kJ/mol) Calculated with MIPp for **H-1**−**H-3** Interacting with Cl^- at Several Distances (Å) from the Center of the Rings

	E_e		E_p		E_{vw}		E_t	
distance	6R	5R	6R	5R	6R	5R	6R	5R
				H-1				
2.5	−358.10	*−366.88*	−62.87	*−59.36*	80.17	*105.80*	−340.75	*−320.44*
2.8	−336.36	*−343.89*	−45.31	*−42.09*	12.33	*17.51*	−369.34	*−368.47*
3.0	−323.45	*−330.01*	−36.83	*−33.98*	−1.55	*0.88*	−361.82	*−363.16*
3.2	−311.54	*−317.18*	−30.14	*−27.71*	−6.48	*−4.97*	−348.15	*−349.91*
3.5	−295.23	*−299.62*	−22.61	*−20.82*	−7.57	*−6.56*	−325.41	*−327.00*
4.0	−271.37	*−274.12*	−14.55	*−13.46*	−5.48	*−4.81*	−291.39	*−292.39*
				H-2				
2.5	−352.33	*−329.26*	−61.66	*−62.70*	74.57	*113.19*	−339.42	*−278.76*
2.8	−331.06	*−312.25*	−44.60	*−44.48*	11.24	*21.03*	−364.41	*−335.74*
3.0	−318.43	*−302.05*	−36.28	*−35.82*	−1.71	*2.63*	−356.43	*−335.24*
3.2	−306.81	*−292.43*	−29.72	*−29.13*	−6.27	*−4.10*	−342.80	*−325.71*
3.5	−290.84	*−279.02*	−22.40	*−21.74*	−7.27	*−6.23*	−320.48	*−307.02*
4.0	−267.52	*−258.78*	−14.46	*−13.92*	−5.23	*−4.72*	−287.21	*−277.43*
				H-3				
2.5	−355.55	*−384.94*	−60.82	*−61.61*	77.41	*102.45*	−338.75	*−344.14*
2.8	−333.98	*−360.94*	−43.76	*−43.93*	12.08	*17.26*	−365.62	*−387.61*
3.0	−321.11	*−346.40*	−35.45	*−35.53*	−1.30	*0.38*	−357.89	*−381.55*
3.2	−309.28	*−332.85*	−28.97	*−28.97*	−6.06	*−5.64*	−344.31	*−367.46*
3.5	−293.02	*−314.13*	−21.69	*−21.69*	−7.15	*−7.27*	−321.86	*−343.09*
4.0	−269.23	*−286.58*	−13.92	*−13.92*	−5.18	*−5.35*	−288.34	*−305.89*

interesting points arise. First, it is worth mentioning that the π interaction of Cl^- with both five- and six-membered rings in compounds **1**−**5** is favorable in a wide range of distances (from 3.0 to 4.0 Å). In all cases, the minimum is found at approximately 3.0 Å from the center of the ring. In adenine compounds **1**, **2**, **4**, and **5** the interaction energy of chloride at the MIPp minimum with the 5R is more favorable than the interaction with the 6R. Second, it is interesting to note the behavior of dimer **4** and bisadenine **5**. The interaction of Cl^- at the 6R of either **4** or **5** is more favorable than **1**, indicating that the anion$-\pi$ interaction through the 6R is reinforced by the presence of the $\pi-\pi$ stacking interaction. In contrast, the interaction at the 5R is almost unaltered in **5** and less favorable in **4**. Third, inspection of the partition energies reveals that the adenine rings are not deficient enough to provide a favorable electrostatic interaction with the anion. The interaction is dominated by the polarization term, which is large and negative, and compensates for the unfavorable electrostatic term. In contrast, interaction of compound **3** with Cl^- at the MIPp minimum has a negative electrostatic term at the 6R due to the presence of the carbonyl group, instead of the $-NH_2$, that increases the electron deficiency of the 6R. The electrostatic term at the 5R is comparable to the rest of the compounds. The van der Waals contribution (dispersion−repulsion) is small and does not have a remarkable influence on the anion$-\pi$ binding.

A likely explanation of the mechanism responsible for interplay between the $\pi-\pi$ and anion$-\pi$ interaction that we found in the adenine dimer **4** and bisadenine **5** can be

(39) (a) Cubero, E.; Luque, F. J.; Orozco, M. *Proc. Natl. Acad. Sci. U.S.A.* **1998**, *95*, 5976. (b) Garau, C.; Frontera, A.; Quiñonero, D.; Ballester, P.; Costa, A.; Deyà, P. M. *Chem. Phys. Chem.* **2003**, *4*, 1344. (c) Garau, C.; Frontera, A.; Quiñonero, D.; Ballester, P.; Costa, A.; Deyà, P. M. *J. Phys. Chem. A* **2004**, *108*, 9423. (d) Garau, C.; Quiñonero, D.; Frontera, A.; Ballester, P.; Costa, A.; Deyà, P. M. *Org. Lett.* **2003**, *5*, 2227. (e) Quiñonero, D.; Garau, C.; Frontera, A.; Ballester, P.; Costa, A.; Deyà, P. M. *Chem. Phys. Lett.* **2002**, *359*, 486. (f) Garau, C.; Quiñonero, D.; Frontera, A.; Escudero, D.; Ballester, P.; Costa, A.; Deyà, P. M. *Chem. Phys. Lett.* **2007**, *438*, 104. (g) Quiñonero, D.; Frontera, A.; Escudero, D.; Ballester, P.; Costa, A.; Deyà, P. M. *Chem. Phys. Chem.* **2007**, *8*, 1182.

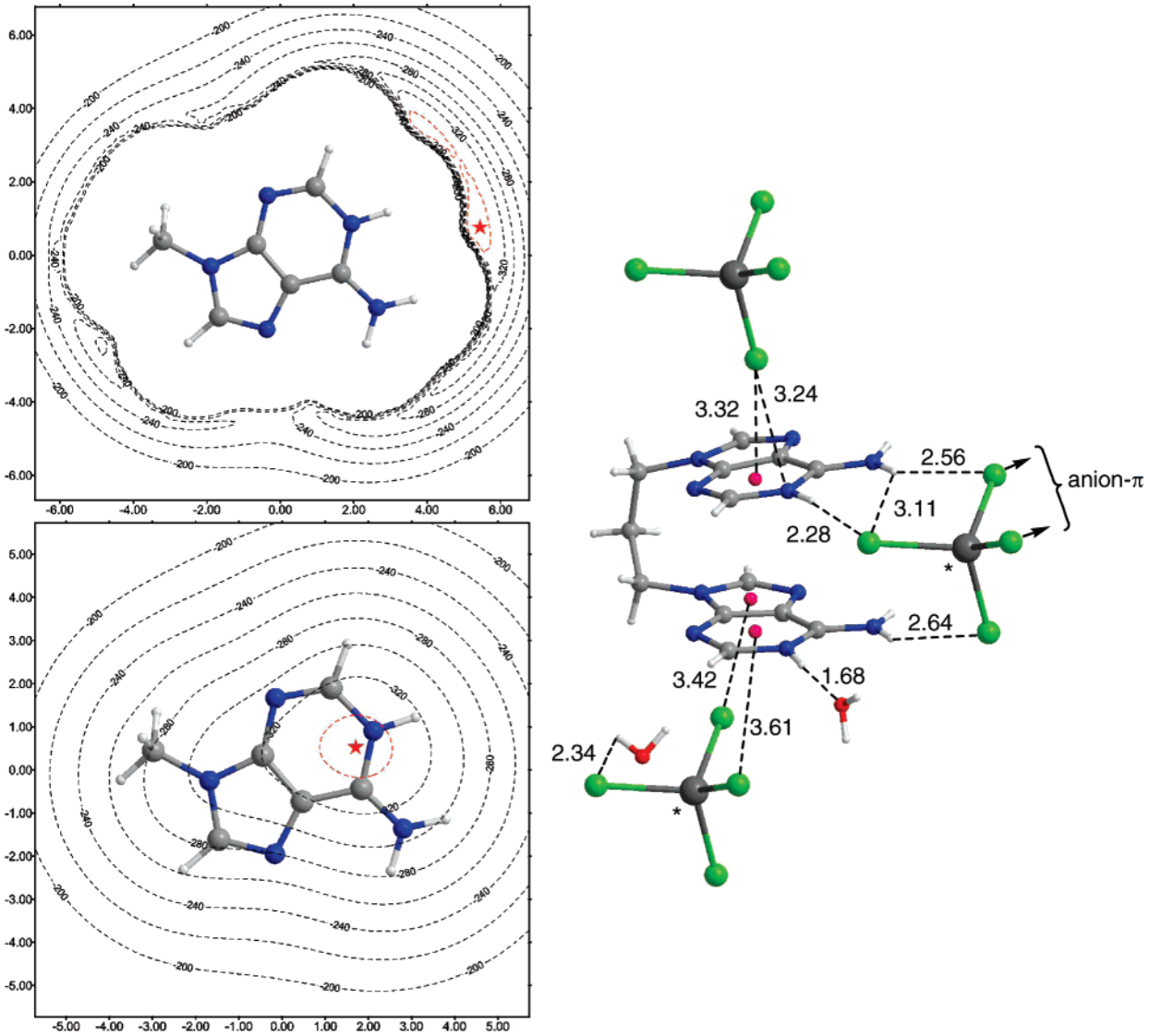

Figure 8. (Left) 2D-MIPp(Cl^-) energy maps of **H-1** at the molecular plane and 3.4 Å above it. Isocontour lines are plotted every 20 kJ/mol. The MIPp minimum of each map is represented by a red star, and the lowest isocontour line is plotted in red. (Right) Partial view of X-ray structure **7**. Distances in Ångstroms.

Scheme 3. Schematic Representation of the Ion-Induced Dipole and Permanent Quadrupole and Their Favorable Interaction in the Ternary Complex

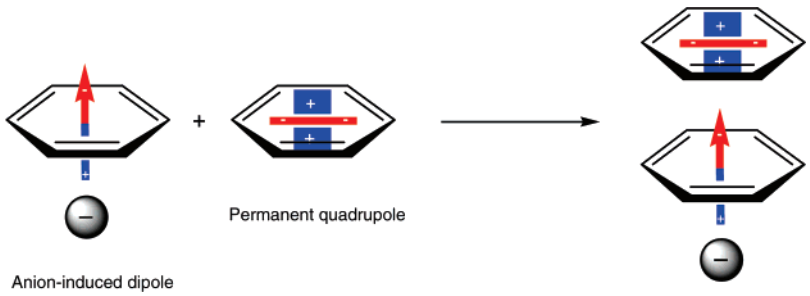

rationalized in terms of electrostatic effects. In Scheme 3 we represent the dipole moment that the anion induces by polarizing the π cloud of an aromatic ring. In the ternary complex a favorable dipole−quadrupole interaction is generated that strengthens the $\pi-\pi$ interaction. An isolated $\pi-\pi$ stacking interaction between aromatics is governed by dispersion effects.[40] In the ternary anion$-\pi-\pi$ complex the stacking is governed by a stronger interaction, leading to an enhancement effect.

To this point we studied and discussed the interaction of neutral adenine and hypoxanthine with chloride. We demonstrated that the interaction in **1** and **2** is energetically favorable due to polarization effects since the aromatic rings of adenine are not π-acidic enough. We have also shown that the interaction via the 5R is more favorable. However,

(40) Sinnokrot, M. O.; Sherrill, C. D. *J. Phys. Chem. A* **2004**, *108*, 10200.

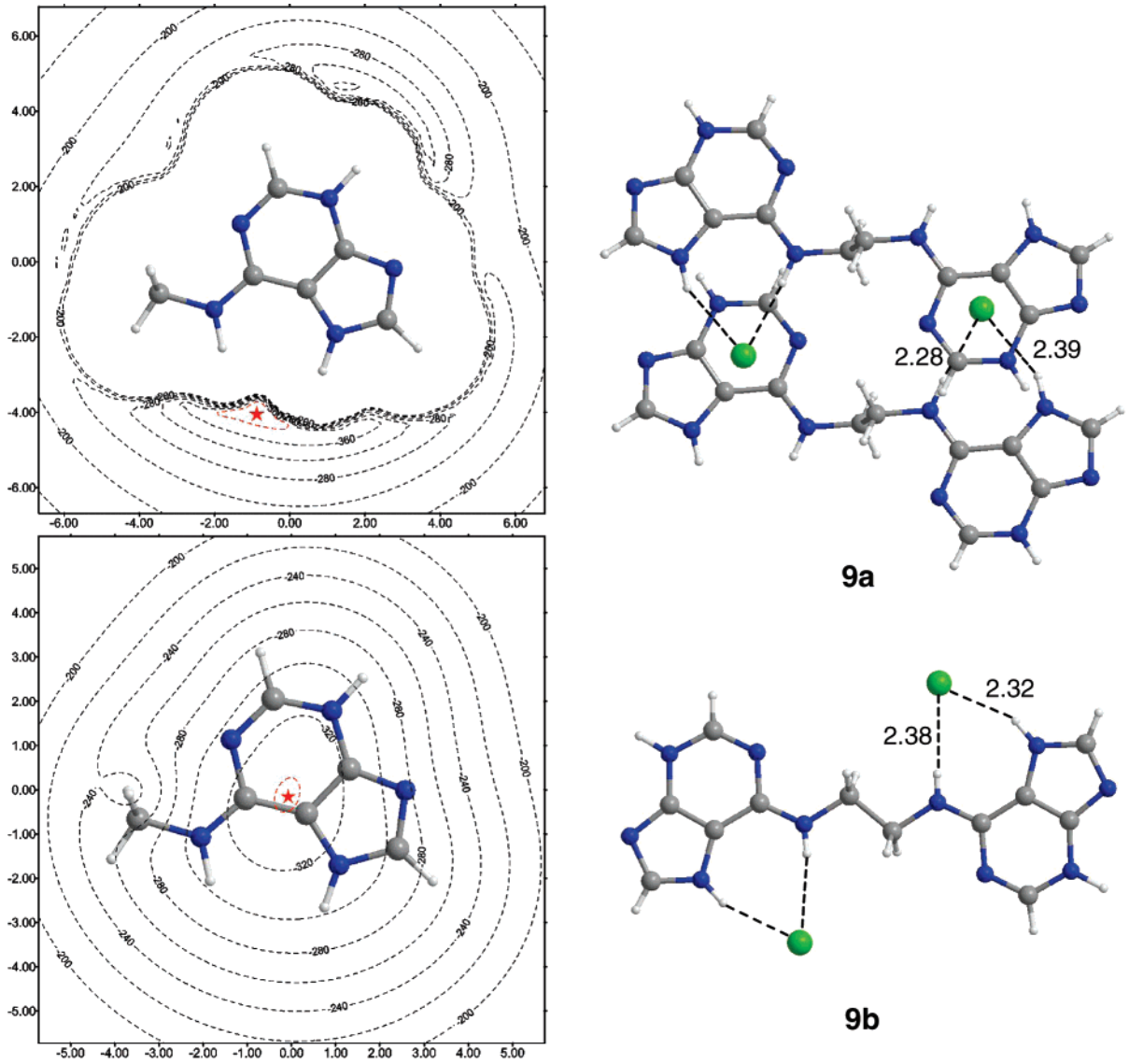

Figure 9. (Left) 2D-MIPp(Cl^-) energy maps of **H-2** at the molecular plane and 3.4 Å above it. Isocontour lines are plotted every 40 kJ/mol in the map computed at the molecular plane and every 20 kJ/mol in the map computed above the molecular plane. The minimum of each map is represented by a red star, and the lowest isocontour line is plotted in red. (Right) Partial views of X-ray structures **9a** and **9b**. Distances in Ångstroms.

in the real compounds reported in this manuscript the counterion of the anion is the adenine (or hypoxanthine) moiety that has one nitrogen atom protonated. Therefore, it is expected that the electrostatic interaction in these systems will be very important. The study of neutral systems is important because it allows demonstration that the ADN bases like adenine are well suited to interact with anions and its capacity via the 6R is incremented when it is participating in $\pi-\pi$ stacking interactions. We extended the energetic study to the protonated forms of **1**−**3** (see Figure 7). The results are summarized in Table 3. As expected, the interaction energies are more favorable in comparison to the neutral forms due to electrostatic effects. The polarization contribution is similar to that computed for neutral compounds (see Tables 2 and 3). It is worth mentioning that in **H-1** the interaction energy of Cl^- with both 5R and 6R rings is similar, indicating that the anion$-\pi$ interaction is more favorable in the 6R ring since in the interaction with 5R there is an additional hydrogen-bond interaction $Cl^-\cdots H_3C-N^9$. This fact is confirmed by analyzing the energetic features of **H-2**, where the interaction of Cl^- with the 6R is more favorable than at the 5R because the methyl group is bonded to N^6 instead of N^9 and the hydrogen bond cannot be formed. In contrast, the interaction of **H-3** with Cl^- is more favorable via the 5R because the protonated nitrogen atom belongs to the 5R.

With the purpose of comparing the anion−binding affinities of compounds **H-1**, **H-2**, and **H-3** via hydrogen bonding and anion$-\pi$ bonding we computed their two-dimensional (2D) MIPp energy maps. We obtained the 2D-MIPp(Cl^-) maps at the molecular plane to study the spatial regions where the σ interaction with Cl^- is more favorable and at 3.4 Å above the molecular plane in order to study where the π interaction with Cl^- is more favorable. In addition, we compared the 2D-MIPp maps with the corresponding X-ray structures. In Figure 8 we show the 2D-MIPp maps calculated for **H-1** and the X-ray structure of **7**. From inspection of the maps the following results are remarkable. First, the global

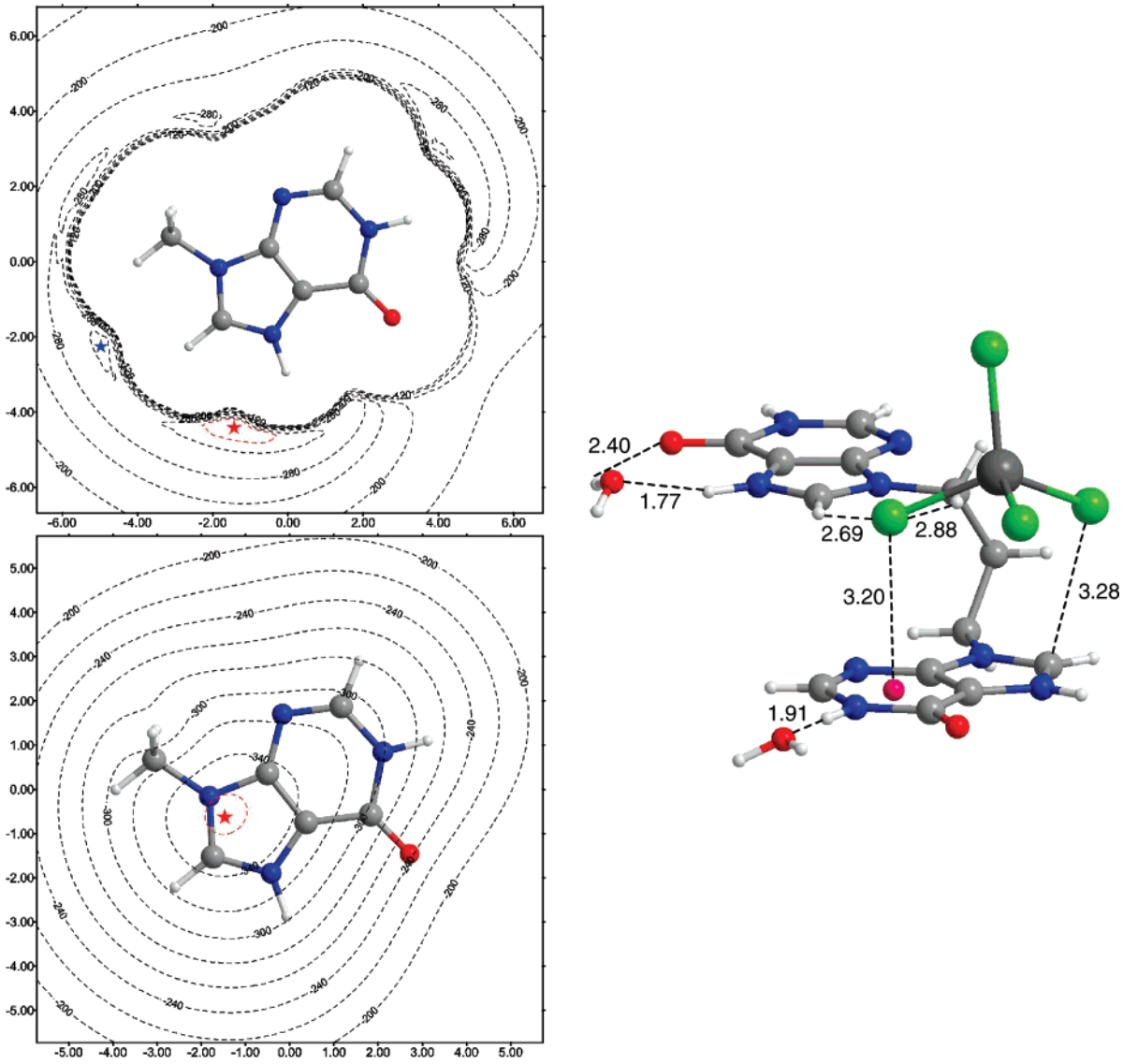

Figure 10. (Left) 2D-MIPp(Cl^-) energy maps of **H-3** at the molecular plane and 3.4 Å above it. Isocontour lines are plotted every 40 kJ/mol in the map computed at the molecular plane and every 20 kJ/mol in the map computed above the molecular plane. The minimum of each map is represented by a red star, and the lowest isocontour line is plotted in red. (Right) Partial view of X-ray structure **10**. Distances in Ångstroms.

minimum at the molecular plane arises from the interaction of the anion with the hydrogen atoms bonded to N^6 and N^1. The energy value at the minimum is −371.6 kJ/mol, which is comparable in energy to the anion−π interaction at either 5R or 6R (see Table 3), indicating that both noncovalent interactions are energetically equivalent in this system. Second, the 2D-MIPp map computed at 3.4 Å above the molecular plane indicates that there is a wide region over the 6R where the interaction with Cl^- is very favored (red contour). It is interesting to note that the X-ray structure is in agreement with the energetic results. In the solid state, two different $ZnCl_4^{2-}$ anions are observed. One of them (marked with an asterisk in Figure 8) interacts via two chlorine atoms with the 5R and 6R rings of one adenine unit, establishing two anion−π interactions. In addition, one chlorine atom of the anion is positioned where the 2D-MIPp at the molecular plane predicts, establishing two hydrogen bonds with N^6 and N^1. The other anion interacts via an anion−π interaction with the 6R of the other adenine unit of the bisadenine. The position of this chlorine atom, which does not participate in any other noncovalent interaction, is in sharp agreement with the position of the MIPp minimum in the 2D-MIPp map computed above the molecular plane.

The 2D-MIPp maps computed for **H-2** and the X-ray structures of **9a** and **9b** are shown in Figure 9. The MIPp minimum at the molecular plane is marked with a red asterisk, and the energetic value is −422.6 kJ/mol, considerably more favorable than the anion−π interaction (see Table 3). The location of the MIPp minimum at the molecular plane coincides with the position of the Cl^- in the solid state in both **9a** and **9b** structures. The energetic difference found in **H-2** between the anion−π and hydrogen-bond interaction may explain the geometric features of the isomorphic form **9b**, where the interaction of the anion with the bisadenine is exclusively done through hydrogen bonds. The 2D-MIPp energy map computed above the molecular plane predicts the position of the minimum approximately above the C^5

atom. The position that the Cl^- anion adopts in **9a** is in good agreement with the theoretical results.

The 2D-MIPp energy maps computed for **H-3** and the X-ray structure of **10** are represented in Figure 10. At the molecular plane, the global MIPp minimum is located in the region of N^7 and the energy value is −392.5 kJ/mol, which is comparable to the energetic values computed for the anion−π interaction at 5R and 6R (see Table 3). In the X-ray structure of **10** a water molecule is located at the region where the MIPp is a minimum (red contour), therefore; this position cannot be occupied by the anion. As an alternative, one chlorine atom of the anion is positioned in a region where a local MIPp minimum is found (marked as a blue star in the map). In the 2D-MIPp map computed above the molecular plane the lowest isocontour line (red contour) is located above the 5R and the MIPp minimum is over the region of N^9, probably due to an additional hydrogen-bond interaction with one hydrogen atom of the methyl group bonded to N^9. There is a wide region (isopotential of −320 kJ/mol) where the interaction of Cl^- is very favorable, which includes the 5R and part of the 6R, which agrees with the X-ray structure of **10** where one chlorine atom of the $ZnCl_4^{2-}$ interacts with the middle of the 6R ring and other chlorine atom with the 5R close to the red isocontour line.

4. Conclusion

The results derived from this study reveal that neutral adenine and hypoxanthine are well suited for interacting favorably with anions via both six- and five-membered rings. In adenine and bisadenine, the anion−π interaction with chloride is more favorable through the five-membered ring due to electrostatic effects. The five- and six-membered rings are not π-acidic enough and the computed electrostatic term is positive, and therefore, the interaction is dominated by polarization effects. In contrast, the computed electrostatic term for the π interaction of Cl^- with the six-membered ring of hypoxanthine is favorable because it is more electron deficient due to the presence of the carbonyl group. When adenine is participating in $\pi-\pi$ stacking interactions, in any of the stacking modes studied in this paper and observed experimentally, its capacity for interacting with Cl^- via the six-membered ring increases. This result confirms the existence of synergistic effects between $\pi-\pi$ and anion−π interactions.

The protonated forms of adenine and hypoxanthine are able to form anion−π complexes very favorably due to electrostatic effects. In these compounds, the anion−π interactions via the six- and five-membered rings are similar energetically. This finding is in agreement with the X-ray structures **7** and **10**, where the anion interacts with both 5R and 6R simultaneously. The 2D-MIPp energy maps are in agreement with the X-ray structures since they are able to predict the spatial regions where the interaction of the anion with the compounds is more favorable. In addition, the hydrogen bonding and anion−π interaction in the protonated forms are energetically comparable, and both determine the geometric features of the crystals.

Experimental Section

Elemental analyses were carried out using a Carlo-Erba model 1106 microanalyzer. Infrared spectra (KBr pellets) were recorded on a Bruker IFS 66. ^1H and ^{13}C NMR spectra were obtained with a Bruker AMX 300 spectrometer. Proton and carbon chemical shifts in dimethyl sulfoxide (DMSO-d_6) were referenced to DMSO-d_6 [^1H NMR, δ(DMSO)= 2.50 ppm. All organic and inorganic reagents (Sigma and Aldrich) were used without further purification.

Suitable crystals of **9a**, **9b**, and **10** were selected for X-ray single-crystal diffraction experiments and mounted at the tips of glass fibers on an Enraf-Nonius CAD4 diffractometer producing graphite-monochromated Mo Kα radiation. After the random search of 25 reflections, the indexation procedure gave rise to the cell parameters. See Table S1 (Supporting Information) for a summary of the crystal data of the three compounds. Data were collected in the $\omega-2\theta$ scan mode. Absorption correction was performed following the PSI scan semiempirical (**9a**) and the empirical DIFABS (**9b** and **10**) methods. The structural resolution procedure was made using the WinGX package.[41] Solving for structure factor phases was performed by SHELXS86[42] (**9a** and **9b**) and SIR2004[43] (**10**), and the full-matrix refinement was by SHELXL97.[44] Non-H atoms were refined anisotropically, and H atoms were introduced in calculated positions and refined riding on their parent atoms. The large residues in **10** are close to Cl23 and may be related with some positional disorder. A summary of the refinement parameters can be also seen in Table S1.

Synthesis of $N^6,N^{6'}$-Dimethylene-bisadenine $(AdeNH)_2(CH_2)_2\cdot 0.75H_2O$ and $N^6,N^{6'}$-Dimethylene-bisadenine Dihydrochloride $[(H\text{-}AdeNH)_2(CH_2)_2][2Cl]$ (9). A suspension of 1 g (6.5 10^{-3} mol) of 6-chloropurine in 20 mL of 1-butanol and 3 mL of triethylamine was refluxed with 0.24 g (4.0×10^{-3} mol) of 1,2-ethylenediamine for 4 h. The resulting solid was filtered off and washed with water and acetone. Further purification can be achieved by recrystallization from boiling water (55%). Anal. Calcd for $C_{12}H_{13}N_{10}\cdot 0.75H_2O$: C, 46.5; H, 4.4; N, 45.2. Found: C, 46.4; H, 4.3; N, 44.8. IR (cm^{-1}): 3207m, 3062s, 2817s, 1624vs, 1597vs, 1543m, 1452m, 1403m, 1339s, 1303s, 1274s, 1252m, 1163m, 1135m, 937s, 906s, 667 m, 651s, 521m. ^1H NMR (DMSO-d_6): δ 8.23 s [2H, Ade-H(2)/Ade-H(2′)], 8.15 s [2H, Ade-H(8)/Ade-H(8′)], 7.79 bs [2H, Ade-H(6)/Ade-H(6′)], 3.73 bt [4H, Ade-CH_2/Ade-CH'_2]. Dissolution of the material in 1 M HCl yields the corresponding hydrochloride [(H-AdeNH)$_2$(CH$_2$)$_2$][2Cl] **9a** (50%). Anal. Calcd for $C_{12}H_{14}Cl_2N_{10}\cdot 0.5H_2O$: C, 38.1; H, 4.0; N, 37.0. Found: C, 38.1; H, 3.9; N, 37.1. IR (cm^{-1}): 3111s, 2774s, 1651vs, 1607s, 1573s, 1514s, 1489m, 1453s, 1424s, 1380s, 1343m, 1296m, 1272s, 1202s, 1158m, 1131m, 893m, 774s, 670m, 613s, 541m. ^1H NMR (DMSO-d_6): δ 9.17 bs [2H, Ade-H(6)/Ade-H(6′)], 8.47 s [2H, Ade-H(2)/Ade-H(2′)], 8.41 s [2H, Ade-H(8)/Ade-H(8′)], 3.88 bt [4H, Ade-CH_2/Ade-CH'_2]. Attempts to prepare the corresponding complex between $N^6,N^{6'}$-dimethylene-bisadenine and $ZnCl_2$ in HCl (1 M) yielded a crop of crystals which correspond to an isomorphic structure of the corresponding dihydrochloride [(H-AdeNH)$_2$(CH$_2$)$_2$][2Cl] **9b**.

Synthesis of $N^9,N^{9'}$-Trimethylene-bishypoxanthine $(Hyp)_2(CH_2)_3\cdot 0.5H_2O$, Precursor of 10. A 0.5 g (1.6 10^{-3} mol) amount

(41) Farrugia, L. J. *J. Appl. Crystallogr.* **1999**, *32*, 837.
(42) Sheldrick, G. M. *SHELXS86, Program for the solution of crystal structures*; University of Göttingen: Göttingen, Germany, 1986.
(43) Burla, M. C.; Caliandro, R.; Camalli, M.; Carrozzini, B.; Cascarano, G. L.; de Caro, L.; Giacovazzo, C.; Polidori, G.; Spagna, R. *J. Appl. Crystallogr.* **2005**, *38*, 381.
(44) Sheldrick, G. M. *SHELXL97, Program for crystal structure analysis* (Release 97-2); University of Göttingen: Göttingen, Germany, 1997.

of N^9,$N^{9'}$-trimethylene-bisadenine[19a] was dissolved in 40 mL of HCl (4 M). The resulting solution was cooled until 4 °C in an ice−water bath. After that a solution of 2 g of $NaNO_2$ ($2.9\ 10^{-3}$ mol) in 2 mL of H_2O was added dropwise. The resulting mixture was heated at 70 °C for 5 min, and then it was allowed to reach room temperature. Subsequently, the pH of the solution was adjusted to 8 using K_2CO_3. The resulting yellow solid was filtered off and washed with water and acetone, yielding the corresponding bishypoxanthine (75%). Anal. Calcd for $C_{13}H_{12}N_8O_2 \cdot 0.5H_2O$: C, 48.6; H, 4.0; N, 34.9. Found: C, 48.7; H, 3.8; N, 35.0. IR (cm^{-1}): 3124m, 3049s, 2860br s, 2806br s, 1696br vs, 1653sh, 1593s, 1548s, 1525m, 1475m, 1446m, 1414s, 1363s, 1345s, 1301w, 1284w, 1259w, 1238w, 1208s, 1194s, 1163w, 1127s, 1070m, 908br m, 856m, 789m, 697m, 646s, 611s, 569w, 528w. This product is insoluble in common deuterated solvents; for this reason NMR spectra were performed in DCl/D_2O. ^1H NMR δ(DCl (1 M)/D_2O): 9.30 bs [2H, Hyp-H(8)/Hyp-H(8′)], 8.31 s [2H, Hyp-H(2)/Hyp-H(2′)], 4.50 t [4H, Hyp-CH_2/Hyp-CH'_2, J: 6.9 Hz], 2.08 br t [2H, Hyp-CH_2–CH_2]. ^{13}C NMR δ(DCl (1 M)/D_2O): 158.8 [Hyp-C(6)/Hyp-C(6′)], 154.1 [Hyp-C(2)/Hyp-C(2′)], 152.1 [Hyp-C(4)/Hyp-C(4′)], 144.5 [Hyp-C(8)/Hyp-C(8′)], 48.0 [Hyp-CH_2/Hyp-$CH_{2'}$], 33.4 [Hyp-CH_2-CH_2].

Synthesis of N^6,$N^{6'}$-Trimethylene-bishypoxanthine Complex with $ZnCl_2$ [(H-Hyp)$_2$(CH_2)$_3$][$ZnCl_4$] (10). 0.09 g (6.6×10^{-3} mol) of $ZnCl_2$ was added to a stirred warm solution (40 °C) of 0.05 g (1.6×10^{-4} mol) of N^9,$N^{9'}$-trimethylene-bishypoxanthine dissolved in 10 mL of HCl (1 M). The resulting solution was kept at this temperature for 30 min and then allowed to stay at room temperature. Crystals of **10** suitable for X-ray were obtained after 1 month. Anal. Calcd for $C_{13}H_{14}Cl_4N_8O_2Zn \cdot 1.5H_2O$: C, 28.5; H, 3.1; N, 20.4. Found: C, 28.5; H, 3.1; N, 20.1. IR (cm^{-1}): 3067br s, 2924br s, 1726br vs, 1700sh, 1603m, 1571s, 1535m, 1510m, 1451w, 1419s, 1376m, 1340m, 1303m, 1263s, 1192w, 1160s, 1129s, 1054w, 975w, 928w, 903m, 866m, 849m, 826m, 779m, 731m, 715w, 679m, 611s, 533m. ^1H NMR δ(DCl (1 M)/D_2O): 9.23 bs [2H, Hyp-H(8)/Hyp-H(8′)], 8.27 s [2H, Hyp-H(2)/Hyp-H(2′)], 4.48 t [4H, Hyp-CH_2/Hyp-CH'_2, $J = 6.7$ Hz], 2.06 br t [2H, Hyp-CH_2-CH_2].

Acknowledgment. We thank the DGICYT of Spain (projects CTQ2005-08989-01 and CTQ2006-09339/BQU) and the Direcció General de Recerca, Desenvolupament Tecnològic i Innovació del Govern Balear (Accions Especials, 2004) for financial support. We thank the CESCA for computational facilities. D.E. thanks the MEC for an undergraduate fellowship. D.Q. thanks the MEC for a "Juan de la Cierva" contract. F.M.A. and M.B.O. acknowledge respective grants of Conselleria d'Economia, Hisenda i Innovació (Govern de les Illes Balears).

Supporting Information Available: Full citation for ref 29, Cartesian coordinates of RI-MP2/6-31++G**-optimized structures **1**−**5**, **H-1**, **H-2**, and **H-3**, crystallographic information files (cif) of new compounds **9a**, **9b**, and **10**, and a summary of the crystal data of the three compounds (Table S1). This material is available free of charge via the Internet at http://pubs.acs.org.

IC701555N